

# Absorption of Microwaves During Plasma Heating at the Second Harmonic of Electron Cyclotron Resonance in Tokamaks and Stellarators: Linear Theory and Experiment

Yu. N. Dnestrovskij<sup>a</sup>, A. V. Melnikov<sup>a,b,c,\*</sup>, V. F. Andreev<sup>a</sup>, S. E. Lysenko<sup>a</sup>,  
M. R. Nurgaliev<sup>a</sup>, and A. G. Shalashov<sup>d</sup>

<sup>a</sup> National Research Center Kurchatov Institute, Moscow, 123182 Russia

<sup>b</sup> National Research Nuclear University MEPhI (Moscow Engineering Physics Institute), Moscow, 115409 Russia

<sup>c</sup> Moscow Institute of Physics and Technology (National Research University),  
Dolgoprudnyi, Moscow region, 141701 Russia

<sup>d</sup> Institute of Applied Physics, Russian Academy of Sciences, Nizhny Novgorod, 603000 Russia

\*e-mail: melnikov\_AV@nrcki.ru

Received June 21, 2023; revised July 20, 2023; accepted July 20, 2023

We study the microwave absorption during electron cyclotron resonance heating (ECRH) by the extraordinary wave at second harmonic (X2 mode) in the T-10 tokamak and TJ-II stellarator in a wide range of plasma densities, and compare experiments with the classical formulas for the absorption of the injected ECR power. Empirical relations for the absorption efficiency and for the critical plasma density  $n_{cr}$ , which separates the regions with full and partial absorption of the injected ECR power, are obtained using the numerical simulation of the heat transport with the transport model of canonical profiles. It is shown that in both devices, the range of densities exists, where the absorption predicted by the classical formulas is almost full, while according with the empirical formula, only a small fraction of the power is absorbed. The obtained relations allow ones to optimize the conditions of ECRH in toroidal systems for magnetic plasma confinement.

DOI: 10.1134/S0021364023602282

## INTRODUCTION

Microwave heating on harmonics of electron cyclotron resonance (ECRH) is one of the most effective methods for additional plasma heating in modern fusion devices with magnetic confinement—tokamaks and stellarators. However, it is known that in the non-relativistic formulation of the equations, microwaves with purely transverse propagation are not absorbed. B.A. Trubnikov in his pioneering work [1] determined the elements of the plasma permittivity tensor in the relativistic formulation. Then it was shown that in the weakly relativistic approximation, the full absorption is realized only for the ordinary mode at the fundamental cyclotron harmonic (O1 mode) and for the extraordinary mode at the second harmonic (X2 mode), while for other modes the absorption is small [2]. Subsequently, these results were generalized to microwaves with arbitrary direction of propagation [3]. Further progress in this problem is described in the reviews [4–7].

Various physical effects that could lead to partial microwave absorption are considered in papers [8–13], however, this problem has not yet been completely solved.

Along with heating of the plasma electrons in tokamaks and stellarators, microwaves can excite or change various types of plasma oscillations, which, in turn, can affect to anomalous transport. Knowledge of the absorbed ECRH power is necessary to establish the properties of these oscillations and to find scalings for their description [14–16], as well as for quantitative modeling of the transport.

In [17–20], the absorption of the X2 mode, propagating perpendicular to the magnetic field, is discussed on the base of experiments in the T-10 tokamak and TJ-II stellarator [19, 21]. General principles of equivalence between discharges in tokamaks and stellarators have been proposed. For a pair of equivalent discharges, the equality of their electron and ion temperatures was shown [19, 21]. The common properties of the energy transport in tokamaks and stellarators were established.

In this paper, we analyze the generally accepted theoretical formula for the plasma optical thickness upon absorption of the X2 mode and compare it with results of the T-10 experiments on heating at the first and second ECR harmonics. From the analysis of these experiments by the Canonical Profile Transport Model (CPTM), an empirical formula for the absorbed microwave power is derived, which is compared with the theoretical formula, and the efficiency of ECRH in the T-10 tokamak and TJ-II stellarator is estimated. Next, we discuss the possibility of transition to full absorption of microwaves. In conclusion, we summarize the main results.

### PLASMA OPTICAL THICKNESS

In the above papers, microwave absorption is usually characterized within the geometric optic approximation in terms of the plasma optical thickness, defined as

$$\tau = \int 2\text{Im}k_s ds, \quad (1)$$

where the integration is performed over the resonant region of the ray path,  $s$  is a coordinate along the ray,  $\text{Im}k_s$  is the imaginary part of the wave vector determined by the solution of the dispersion equation

$$D(\omega, k) = 0, \quad (2)$$

where  $D$  is a plasma dielectric permittivity tensor. The fraction of absorbed power is determined by the expression

$$\eta = 1 - \exp(-\tau). \quad (3)$$

Here, we restrict ourselves to the case of the X2 mode propagation across the magnetic field. We consider an approximate expression for the plasma optical thickness from [4]:

$$\tau_{X_2} = \pi \frac{\omega_p^2}{\omega_B^2} \frac{T_e}{mc^2} \mu_2^X \frac{\omega_B R}{c}. \quad (4)$$

Here,  $\omega_p^2 = 4\pi ne^2/m$  is the squared plasma frequency,  $\omega_B = eB/mc$  is the electron cyclotron frequency. The values of the plasma density and magnetic field in integration of (1) are taken in the resonant zone. Away from the cutoff density, the parameter  $\mu_2^X$  is varied in the range from 1.1 to 1.3.

Let us rewrite Eq. (4) in practical units: the density  $n$  in [ $10^{19} \text{ m}^{-3}$ ], the electron temperature  $T_e$  in keV, and the magnetic field  $B$  in Teslas. Thus,  $T_e/mc^2 = T_e [\text{keV}]/511$ , and (4) has a form

$$\tau_{X_2} \approx 5.6 \frac{n T_e R}{B \cdot 1.5}. \quad (5)$$

Here, we normalized the major radius of a tokamak  $R$  to the major radius of the T-10 device ( $R_{T-10} = 1.5 \text{ m}$ ).

We set  $\mu_2^X = 1$  that gives the accuracy of the optical thickness estimation as 10–30%.

### ANALYSIS OF EXPERIMENTAL RESULTS

The microwave absorption at the first and second ECR harmonics in the T-10 tokamak is considered in [17, 18]. Quantitative analysis of the ECRH using CPTM led to the following conclusions [18–20]. Although the optical thickness at the fixed magnetic field depends not only on the density, but also on the electron temperature, so, at sufficiently high average density  $n$ , the full absorption of microwaves takes place. At sufficiently low density, absorption may become partial. We call the boundary of the transition from partial to full absorption as the critical density  $n_{\text{cr}}$ .

So, if

$$n > n_{\text{cr}}, \quad (6)$$

the absorption is full, independently of the electron temperature. Otherwise, if

$$n < n_{\text{cr}}, \quad (7)$$

the absorption depends on the value of the partial electron pressure  $p_e$ . If the condition (7) is satisfied, but if the electron pressure is sufficiently high:

$$p_e = n T_e > 8.8 (R_{T-10}/R), \quad (8)$$

then the full absorption of the microwave is preserved, since the optical thickness increases due to the temperature. If the condition (7) is fulfilled and the electron pressure is low:

$$p_e = n T_e < 8.8 (R_{T-10}/R), \quad (9)$$

then the absorption remains partial.

Results of analysis from [18–21] are collected in Fig. 1. Here, on the plane (density–electron temperature), shots with ECRH at the fundamental O mode (O1) and at the second harmonic X mode (X2) are shown. Under ECRH at the first harmonic [22], in this area, the temperature  $T_e$  rapidly increases with decreasing density. A sharp difference in temperatures is seen, when the low-density plasma,  $n < 3 \times 10^{19} \text{ m}^{-3}$ , is heated. Under ECRH at the second harmonic, the temperature also increases, but very slowly. As a result, at the density of  $n \sim 2$ , the temperatures differ in a factor of 4–5. We suppose that such a difference owing to partial absorption of the X2 mode.

The blue line in Fig. 1 marks the boundary between areas of full and partial absorption (8). It describes the empirical condition of full absorption obtained for T-10 (see condition (5) from [19]):

$$n_0 T_{e0} > 10 [10^{19} \text{ m}^{-3} \text{ keV}], \quad (10)$$

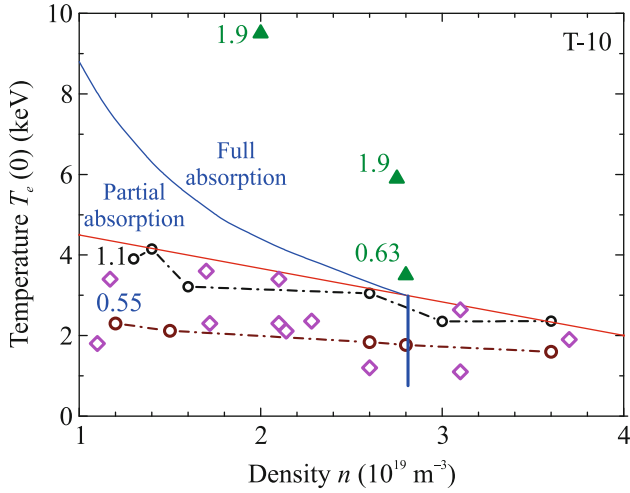


**Fig. 1.** (Color online) Comparison of ECRH at the first and second harmonics in the T-10 tokamak. Green triangles mark heating at the first harmonic O1 mode at  $B = 2.8$  T,  $f = 75\text{--}81.4$  GHz [22]. The heating power for each shot is shown. Below the red line, the area of temperatures obtained in the 2013–2018 campaigns in shots with ECRH at the X2 mode within the power range  $0.4 < Q_{EC} < 2.3$  MW (open symbols) lies [19]. Circles and dash-dotted lines mark two series of shots with heating power  $Q_{EC} \sim 1.1$  and  $0.55$  MW,  $B = 2.32$  T and the carbon limiter. Blue line ( $T_e = 8.8/n$ ) divides areas of partial and full absorption;  $n_{cr} = 2.8 \times 10^{19} \text{ m}^{-3}$ .

where  $n_0$  and  $T_{e0}$  are the central electron density and temperature. A more detailed analysis of the experimental data shows that the factor 10 in relation (10) should be reduced to 8.8, and the central value of the plasma density may be replaced by the average value without large errors. Thus, for the boundary of the full absorption area, we obtain the dependence shown by the blue line in Fig. 1:

$$T_e = 8.8/n. \quad (11)$$

Two series of shots with different densities and different ECRH powers of 1.1 and 0.55 MW (circles and dash-dotted lines in Fig. 1) are very interesting as well. We see that the electron temperature in these series increases very slightly with decreasing density. It confirms our assumption that the efficiency of microwave absorption decreases with decreasing density. Note that the position of the experimental points at the power of 1.1 MW for this series practically coincides with the upper limit for the electron temperatures reached in experiments with heating power of 0.4 to 2.3 MW (see Fig. 5 in [19]), marked by the red line in Fig. 1. This occurs because the experimental series with a power of 1.1 MW were carried out in shots with a carbon limiter. Later, when the power of the gyrotrons at the device reached 2.3 MW, the carbon limiter

was replaced by a tungsten limiter. With such a limiter, the electron temperature turned out to be lower than with the carbon limiter. Recall that in the 1980s, when heating from gyrotrons was carried out at the first ECR harmonic, the limiter was carbon also.

So, Fig. 1 demonstrates the effect of reducing microwave absorption with decreasing density, both in regimes with different heating power, and in regimes with different limiter materials.

Figure 1 shows that at the average density  $n = 2 \times 10^{19} \text{ m}^{-3}$ , the additional plasma heating by 1.5 keV allows us to increase the optical plasma density so much that absorption becomes full. For this, we may use some other method of additional heating, for example, neutral beam injection (NBI). As a result, the electron temperature can be high enough to satisfy the condition of full absorption (8). After that, additional NBI heating can be turned off, but the plasma will remain in the area of full absorption. Of course, the considered process is highly non-linear, since the transition through the blue curve is accompanied by transition from partial to full absorption of waves. In the area below the blue curve, absorption depends linearly on density [19], while in the area above the blue curve, absorption is full and independent of density.

Analysis of experimental data using CPTM [17–21] shows that the absorbed power fraction  $\eta = Q_{ab}/Q_{EC}$  in case (7), (9) increases linearly with plasma density. Here,  $Q_{ab}$  is the absorbed power,  $Q_{EC}$  is the injected power. Thus, the complete refined empirical formula for the absorbed power fraction is:

$$\left. \begin{aligned} \eta &= n/n_{cr} & \text{at } n < n_{cr} \text{ and } (nT_e) \leq 8.8(R_{T-10}/R) \\ \eta &= 1 & \text{at } n < n_{cr} \text{ and } (nT_e) > 8.8(R_{T-10}/R) \\ \eta &= 1 & \text{at } n > n_{cr} \\ \eta &= 0 & \text{at } n > n_{cutoff} \end{aligned} \right\}. \quad (12)$$

The empirical relation for the critical density is [19]:

$$n_{cr} = 1.2B. \quad (13)$$

Relation (13) links the boundary of the transition from full to partial absorption with the magnetic field. For T-10 with a field  $B = 2.4$  T, the critical density is about  $2.8 \times 10^{19} \text{ m}^{-3}$ . In [21], we studied the absorption of X2 mode at the second harmonic in the TJ-II stellarator, where the critical density is  $n_{cr} = 1.2 \times 10^{19} \text{ m}^{-3}$  for the field  $B = 1$  T.

Note that relations (8) and (9) are valid for the toroidally symmetric systems (tokamaks), but not always valid for stellarators with different topology of

magnetic field. For stellarators, instead of  $R$ , it is more correct to write  $B/(dB/ds)$ , where the vector  $s$  is parallel to the ray of microwaves.

### COMPARISON OF EMPIRICAL AND CLASSICAL EXPRESSIONS FOR THE OPTICAL THICKNESS AT THE SECOND ECR HARMONIC (X2)

The plasma optical thickness in practical units is given by Eq. (5), and the fraction of absorbed power  $\eta$  is described by the classical expression (3). Now we should compare formulas (3)–(5) with empirical relations (12) and (13).

First, we compare these expressions at low density. Assuming that

$$\tau_{X2} \ll 1, \quad (14)$$

and using the expansion of the exponent in a small argument ( $\exp(x) \sim 1 + x$ ), we obtain for T-10 and TJ-II:

$$\eta = \tau_{X2} = 5.6 \frac{nT_e}{B}. \quad (15)$$

For convenience of comparison, we rewrite formula (12), taking into account (13):

$$\eta = n/1.2B. \quad (16)$$

Expressions (15) and (16) distinguish both in the numerical factor by 6.7 and in parametric scalings. The classical formula (15) contains the electron temperature  $T_e$ , which is absent in relation (16). The large difference in the numerical factor means that the slope of the straight line vs density in (15) is much steeper than in (16). Physically, this means that the area with partial absorption in case (15), although it exists, but it is very small. Apparently, for this reason, this effect was not considered in the published theoretical works.

The dependence of  $\eta$  on the magnetic field in (15) is also distorted due to the presence of an increased numerical factor. If in (16) the critical density is determined by relation (13) ( $n_{cr} = 1.2B$ ), then in (15) it has the form:

$$n_{cr} = B/(5.6T_e), \quad (17)$$

which is much less.

In T-10 shots with density  $n < n_{cr}$ , the electron temperature varies arbitrarily in the range  $2.1 < T_e < 3.6$  keV, i.e., in a factor of 1.7 [18]. In accordance with (15), the experimental points along the line  $\eta(n)$  should be scattered over an area of such a width. However, the scatter of points is much narrower (see Fig. 12 in [19]) that indicates to independence of  $\eta$  on the temperature in experiment.

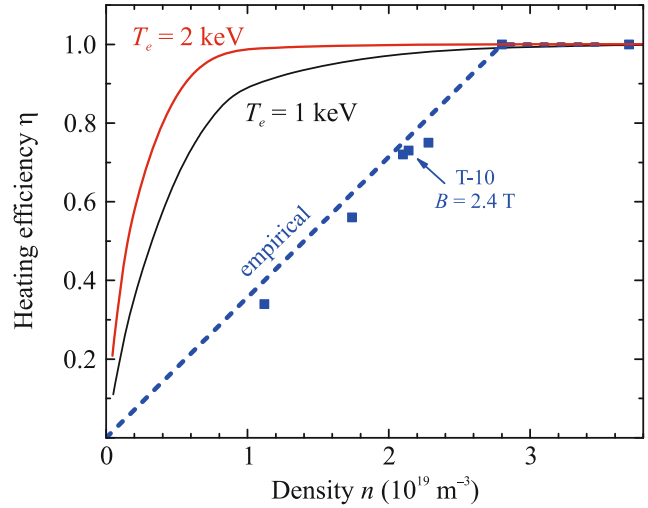


**Fig. 2.** (Color online) Efficiency of ECRH on the density in the T-10 tokamak at the magnetic field 2.4 T. Solid curves correspond to theoretical formulas (4), (5) at temperatures of 1 and 2 keV. The dash broken line corresponds to the empirical formula (12). The blue squares mark the values of heating efficiency for shots with various densities and heating powers for temperatures of 1 and 2 keV [19].

Now we compare the classical formula (3) for  $\eta$  with the empirical formula (12) in a wide density range. We use formula (15) as the argument of the exponent. Figure 2 shows the dependence of the heating efficiency on the plasma density for the T-10 tokamak with magnetic field  $B = 2.4$  T. Lines with saturation correspond to theoretical formulas (3)–(5) at temperatures  $T_e(0) = 1$  and 2 keV. The dashed broken line corresponds to the empirical formula (12). Blue squares mark the values of heating efficiency for T-10 shots with various densities and heating powers. We see that at the indicated magnetic field, the discrepancies between the classical formula (3) and the empirical formula (12) are in the range of density variation

$$0 < n < 2.8 \times 10^{19} \text{ m}^{-3}. \quad (18)$$

For example, at a density of  $n = 1.4 \times 10^{19} \text{ m}^{-3}$ , according to the classical formula, almost whole ECRH power is absorbed, and according to the empirical formula, only half of it.

Figure 3 shows the heating efficiency versus density for the TJ-II stellarator with  $B = 1$  T, obtained with CPTM. In simulations of TJ-II shots, equivalent tokamak discharges were used. The equivalence conditions were defined in [21]. According to (13), the critical density at the indicated magnetic field is  $n_{cr} = 1.2 \times 10^{19} \text{ m}^{-3}$ , so the discrepancy between formulas (3), (4), and (12) are in the range

$$0 < n < 1.2 \times 10^{19} \text{ m}^{-3}. \quad (19)$$

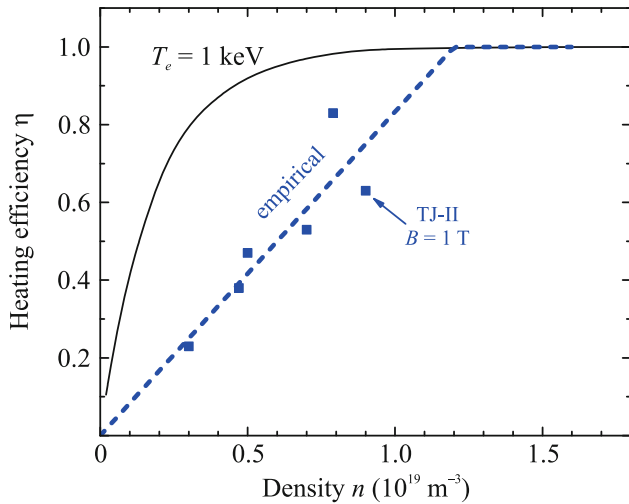


**Fig. 3.** (Color online) Efficiency of ECRH on the density in the TJ-II stellarator at the magnetic field 1 T. Solid curve corresponds to theoretical formulas (4), (5) at the temperature 1 keV. The dash broken line corresponds to the empirical formula (12). The blue squares mark the values of heating efficiency for shots with various densities and heating powers [21]. All experimental points lie in the area of partial absorption.

Symbols mark experimental points of TJ-II I. Since the cutoff density  $n_{\text{cutoff}} = 1.6 \times 10^{19} \text{ m}^{-3}$  at a  $B = 1 \text{ T}$ , then really all experimental points lie in the area of partial absorption (19).

### OVERCOMING THE AREA WITH PARTIAL ABSORPTION

It was shown in [17] that existence of area with partial absorption is associated with the effect of the “temperature threshold” (insufficient electron temperature). If this threshold is exceeded, then the absorption becomes full even at densities below the critical value (condition (7)). The condition for overcoming the threshold (8) requires an increase in the electron pressure. If the condition (8) is not satisfied with the available ECRH power, then there are two ways to achieve full absorption. The first way is to increase the input power  $Q_{EC}$ . Since the fraction of absorbed power remains unchanged at a constant plasma density, an increase in  $Q_{EC}$  will also lead to an increase in the absorbed power  $Q_{ab}$ . The W7-X stellarator team followed to this way, increasing the absorbed power up to 5 MW. At this power, the temperature threshold is overcome and full absorption is achieved. The second way is to use additional power of a different nature. Most frequently, the additional heating by neutral beam injection (NBI) is used (DIII-D [23] and ASDEX-Upgrade [24] tokamaks). The EAST

tokamak uses additional heating by lower hybrid power injection [25]. In many cases, only pulsed input of additional power with a duration of tens milliseconds is used. In transition to full absorption regime (8), the existing ECRH power is sufficient yet to maintain a steady state with a high electron temperature without returning to regime (9) with partial absorption.

To overcome the area of partial absorption, we can also increase the major radius of the device, leading to a corresponding increase in the optical thickness, see the factor  $R/1.5$  in (5), or increase the size of the resonant region. This feature was realized in the W7-X stellarator that has the major radius  $R_{W7-X} = 5.5 \text{ m}$  ( $R_{W7-X}/1.5 = 3.7$ ).

The T-15MD tokamak has  $R = 1.5 \text{ m}$ , and it will operate at magnetic fields  $B = 1\text{--}2 \text{ T}$  [26], i.e., with parameters, comparable to T-10 and TJ-II, therefore, the partial absorption is also possible there [19]. For transition to the full absorption regime, it will be possible to use NBI or ion-cyclotron resonance heating [27, 28]. It is also possible to organize a special scenario, in which the discharge starts at a density slightly higher than the critical one with full absorption, and then to decrease density with a small remaining heating. Then the condition (8) will be satisfied and the electron temperature remains above the blue curve in Fig. 1.

### CONCLUSIONS

An analysis of experiments in the T-10 tokamak and TJ-II stellarator has shown that at the sufficiently low density, the ECRH power at the second harmonic of extraordinary wave (X2 mode) is only partially absorbed. The empirical scaling is constructed for the fraction of the absorbed power as the function of the plasma density, magnetic field, and electron temperature. Its comparison with the classical formulas for the plasma optical thickness and for the fraction of the absorbed ECRH power has shown that the density range with partial absorption also exists in the classical description of the microwave absorption. Examples from the T-10 tokamak and the TJ-II stellarator have shown that this density range is an order of magnitude smaller than that determined by the empirical scaling. The value of the necessary increase in the electron temperature for the transition to the area of full absorption of the ECRH power at the X2 mode is estimated.

### FUNDING

This work was partly supported by the Russian Science Foundation (project no. 23-72-00042).

## CONFLICT OF INTEREST

The authors declare that they have no conflicts of interest.

## OPEN ACCESS

This article is licensed under a Creative Commons Attribution 4.0 International License, which permits use, sharing, adaptation, distribution and reproduction in any medium or format, as long as you give appropriate credit to the original author(s) and the source, provide a link to the Creative Commons license, and indicate if changes were made. The images or other third party material in this article are included in the article's Creative Commons license, unless indicated otherwise in a credit line to the material. If material is not included in the article's Creative Commons license and your intended use is not permitted by statutory regulation or exceeds the permitted use, you will need to obtain permission directly from the copyright holder. To view a copy of this license, visit <https://creativecommons.org/licenses/by/4.0/>.

## REFERENCES

1. B. A. Trubnikov, in *Plasma Physics and the Problem of Controlled Thermonuclear Reactions*, Ed. by M. A. Leontovich (Pergamon, London, 1960), Vol. 4, p. 363.
2. Y. N. Dnestrovskii, D. P. Kostomarov, and N. V. Skrydlov, *Sov. Phys. Tech. Phys.* **8**, 691 (1964).
3. I. P. Shkarofsky, *Phys. Fluids* **9**, 570 (1966). <https://doi.org/10.1063/1.1761711>
4. M. Bornatichi, *Plasma Phys.* **24**, 629 (1982). <https://doi.org/10.1088/0032-1028/24/6/005>
5. M. Bornatichi, R. Cano, O. de Barbier, and F. Engelman, *Nucl. Fusion* **23**, 1153 (1983). <https://doi.org/10.1088/0029-5515/23/9/005>
6. V. V. Alikae, A. G. Litvak, E. V. Suvorov, and A. A. Fraiman, in *High-Frequency Plasma Heating*, Ed. by A. G. Litvak (Am. Inst. Phys., New York, 1992), p. 1. <https://link.springer.com/book/9780883187654>
7. R. Prater, *Phys. Plasmas* **11**, 2349 (2004). <https://doi.org/10.1063/1.1690762>
8. G. Giruzzi, *Nucl. Fusion* **28**, 1413 (1988). <https://doi.org/10.1088/0029-5515/28/8/009>
9. A. G. Shalashov and E. V. Suvorov, *Plasma Phys. Rep.* **28**, 46 (2002). <https://doi.org/10.1134/1.1434295>
10. A. G. Shalashov and E. V. Suvorov, *Plasma Phys. Control. Fusion* **45**, 1779 (2003). <https://doi.org/10.1088/0741-3335/45/9/314>
11. E. Z. Gusakov and A. Yu. Popov, *Phys. Usp.* **63**, 365 (2020). <https://doi.org/10.3367/UFNe.2019.05.038572>
12. E. Z. Gusakov and A. Yu. Popov, *J. Exp. Theor. Phys.* **127**, 155 (2018). <https://doi.org/10.1134/S1063776118070063>
13. E. Z. Gusakov and A. Yu. Popov, *JETP Lett.* **109**, 689 (2019). <https://link.springer.com/article/10.1134/S0021364019110080>
14. A. V. Melnikov, L. I. Krupnik, E. Ascasibar, et al., *Plasma Phys. Control. Fusion* **60**, 084008 (2018). <https://doi.org/10.1088/1361-6587/aac97f>
15. A. V. Melnikov, V. A. Vershkov, S. A. Grashin, M. A. Drabinskij, L. G. Eliseev, I. A. Zemtsov, V. A. Krupin, V. P. Lakhin, S. E. Lysenko, A. R. Nemets, M. R. Nurgaliev, N. K. Khartchev, P. O. Khabanov, and D. A. Shelukhin, *JETP Lett.* **115**, 324 (2022). <https://doi.org/10.1134/S0021364022200279>
16. G. A. Sarancha, L. G. Eliseev, Ph. O. Khabanov, N. K. Kharchev, and A. V. Melnikov, *JETP Lett.* **116**, 98 (2022). <https://doi.org/10.31857/S1234567822140051>
17. Y. N. Dnestrovskij, V. A. Vershkov, A. V. Danilov, A. Yu. Dnestrovskij, S. E. Lysenko, A. V. Melnikov, G. F. Subbotin, D. Yu. Sychugov, S. V. Cherkasov, and D. A. Shelukhin, *Plasma Phys. Rep.* **45**, 226 (2019). <https://doi.org/10.1134/S1063780X19020053>
18. Yu. N. Dnestrovskij, A. V. Danilov, A. Yu. Dnestrovskij, L. A. Klyuchnikov, S. E. Lysenko, A. V. Melnikov, A. R. Nemets, M. R. Nurgaliev, G. F. Subbotin, N. A. Soloviev, A. V. Sushkov, D. Yu. Sychugov, and S. V. Cherkasov, *Plasma Phys. Rep.* **46**, 477 (2020). <https://doi.org/10.1134/S1063780X20050037>
19. Yu. N. Dnestrovskij, A. V. Danilov, A. Yu. Dnestrovskij, S. E. Lysenko, A. V. Melnikov, A. R. Nemets, M. R. Nurgaliev, G. F. Subbotin, N. A. Soloviev, D. Yu. Sychugov, and S. V. Cherkasov, *Plasma Phys. Control. Fusion* **63**, 055012 (2021). <https://doi.org/10.1088/1361-6587/abdc9b>
20. Yu. N. Dnestrovskij, A. V. Danilov, A. Yu. Dnestrovskij, S. E. Lysenko, A. V. Melnikov, A. R. Nemets, M. R. Nurgaliev, G. F. Subbotin, N. A. Soloviev, D. Yu. Sychugov, and S. V. Cherkasov, *Phys. At. Nucl.* **85**, S34 (2022). <https://doi.org/10.1134/S1063778822130051>
21. Yu. N. Dnestrovskij, A. V. Melnikov, D. Lopez-Bruna, A. Yu. Dnestrovskij, S. V. Cherkasov, A. V. Danilov, L. G. Eliseev, F. O. Khabanov, S. E. Lysenko, and D. Yu. Sychugov, *Plasma Phys. Control. Fusion* **65**, 015011 (2023). <https://doi.org/10.1088/1361-6587/aca35a>
22. V. V. Alikae, A. A. Bagdasarov, N. L. Vasin, Yu. N. Dnestrovskij, Yu. V. Esipchuk, A. Ya. Kislov, G. E. Notkin, K. A. Razumova, V. S. Strelkov, and K. N. Tarasyan, *Plasma Phys. Rep.* **14**, 601 (1988).
23. C. C. Petty and the DIII-D Team, *Nucl. Fusion* **59**, 112002 (2019). <https://doi.org/10.1088/1741-4326/ab024a>

24. U. Stroth, J. Adamek, L. Aho-Mantila, et al., *Nucl. Fusion* **53**, 104003 (2013).  
<https://doi.org/10.1088/0029-5515/53/10/104003>
25. J. W. Liu, Q. Zang, Y. Liang, et al., *Nucl. Fusion* **63**, 016011 (2023).  
<https://doi.org/10.1088/1741-4326/aca168>
26. A. V. Melnikov, A. V. Sushkov, A. M. Belov, et al., *Fusion Eng. Des.* **96–97**, 306 (2015).  
<https://doi.org/10.1016/j.fusengdes.2015.06.080>
27. J. Ongena, A. M. Messiaen, A. V. Melnikov, R. Ragona, Ye. O. Kazakov, D. van Eester, Yu. N. Dnestrovskii, P. P. Khvostenko, I. N. Roy, and A. N. Romannikov, *Fusion Eng. Des. A* **146**, 787 (2019).  
<https://doi.org/10.1016/j.fusengdes.2019.01.080>
28. A. V. Melnikov, J. Ongena, A. M. Messiaen, R. Ragona, A. V. Sushkov, Ye. O. Kazakov, D. van Eester, Yu. N. Dnestrovskii, P. P. Khvostenko, and I. N. Roy, *AIP Conf. Proc.* **2254**, 070007 (2020).  
<https://doi.org/10.1063/5.0014265>